

OPEN

Study of Structural stability and formation mechanisms in DSPC and DPSM liposomes: A coarse-grained molecular dynamics simulation

H. Hashemzadeh¹, H. Javadi² & M. H. Darvishi^{2*}

Liposomes or biological vesicles can be created from cholesterol, phospholipid, and water. Their stability is affected by their phospholipid composition which can influence disease treatment and drug delivery efficacy. In this study, the effect of phospholipid type on the formation and stability of liposomes using coarse-grained molecular dynamics simulations is investigated. For this purpose, the simulation study of the DSPC (1,2-distearoyl-sn-glycero-3-phosphocholine) and DPSM (Egg sphingomyelin) lipids were considered. All simulations were carried out using the Gromacs software and Martini force field 2.2. Energy minimization (3000 steps) model, equilibrium at constant volume to adjust the temperature at 400 Kelvin and equilibrium at constant pressure to adjust the pressure, at atmospheric pressure (1 bar) have been validated. Microsecond simulations, as well as formation analysis including density, radial distribution function, and solvent accessible surface area, demonstrated spherical nanodisc structures for the DPSM and DSPC liposomes. The results revealed that due to the cylindrical geometric structure and small-size head group, the DSPC lipid maintained its perfectly spherical structure. However, the DPSM lipid showed a conical geometric structure with larger head group than other lipids, which allows the liposome to form a micelle structure. Although the DSPC and DPSM lipids used in the laboratory tests exhibit liposome and micelle behaviors, the simulation results revealed their nanodisc structures. Energy analysis including overall energy, Van der Waals interaction energy, and electrostatic interaction energy showed that DPSM liposome is more stable than DSPC liposome.

Liposomes, or small vesicles, can be created from non-toxic (normal) cholesterol and phospholipids. Liposomes were introduced in 1965 and initially used as models for studying biological membranes¹. Later, Liposomes have been considered as drug delivery systems. Solutions of phospholipids in water exhibit a large variety of aggregation states such as double layer or liposome membrane^{2,3}. Characteristics such as inherent low toxicity, biodegradability and lack of immunogenicity qualify Liposomes as a considerable carrier in novel drug delivery systems⁴⁻⁷. In addition, Liposomes are dynamic, so different structures can be achieved depending on the phospholipids types^{8,9}. It is now possible to engineer a wide variety of sizes, phospholipids, and liposomal superficial properties¹⁰.

The liposomal surface can be engineered and functionalized by selecting special lipids, in facilitating covalent binding of proteins (e.g. antibodies and proteins to sugars, *i.e.* lectin), glycoproteins and synthetic proteins¹¹. Liposomes are widely used in vaccines, enzymes and drug (insulin and anticancer drugs) carriers¹². In general, the highly unsaturated phospholipid compounds can lead to the instability of the liposome structure¹³. Lipids derived from biological sources such as eggs and soybeans typically consist of significant levels of unsaturated fatty acids, thus inherently are less stable than their counterparts. While saturated lipids are more stable, they have a higher transition temperature¹⁴. Liposomes containing saturated phospholipids showed increased stability and high transition temperature compared to liposomes composed of unsaturated phospholipids. Hence, to liposome synthesizing purposes if unsaturated phospholipids is essential, it is important that keep the transition temperature degree as low as possible. The existence of Polyethylene Glycol (PEG) on the surface of liposomal

¹Nanobiotechnology Department, Faculty of Bioscience, Tarbiat Modares University, Tehran, Iran.

²Nanobiotechnology Research Center, Baqiyatallah University of Medical Sciences, Tehran, Iran. *email: darvishi@alumnus.tums.ac.ir

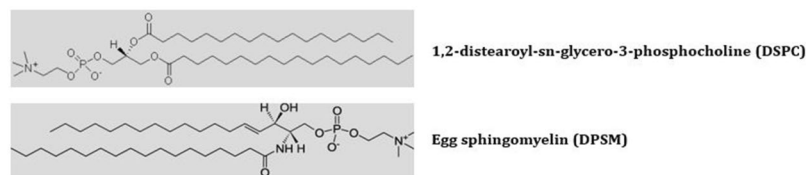


Figure 1. 1,2-distearoyl-sn-glycero-3-phosphocholine and Egg sphingomyelin phospholipids.

delivery systems has shown to increase the half-life in blood-circulation¹⁵, while reducing toxicity and exposure of healthy cells to drug toxicity, i.e. drugs in vulnerable tissues such as the liver and kidneys^{16–19}. In addition, the combination of PEG with liposome has resulted in improvement of liposomal stability^{15,20}. The most important obstacle in liposomal technology is their long-term instability, especially when used as drug carriers²¹. Physical and chemical stability of liposomes are affected by various factors influencing the liposomes stability and the effectiveness of drug penetration²². For this reason, the stability of liposomes is critical for long time circulation. Long-term stability of liposomes containing pharmaceutical substances is strongly influenced by the type of phospholipid's liposome structure.

The main advantage of molecular dynamic simulations is obviously the decreased costs²³. Molecular dynamics simulation is useful tools that offer information about biomolecular hydrodynamic behavior^{9,15}. In other words, fundamental understandings about stability and formation mechanisms of lipids especially liposomes could provide a guideline for rational design of them. Molecular dynamics simulation is helpful to open the new opportunities to further investigate liposomes structure and functionality. Coarse-grained (CG) models offer simulation of larger systems like lipids for longer times by decreasing the number of degrees of freedom (df) compared with all-atom models²³.

In this research, the effect of phospholipid type on the formation and stability of liposomes using coarse-grained molecular simulations is studied. For this purpose, the liposomes of DSPC (1,2-distearoyl-sn-glycero-3-phosphocholine) and DPSM (Egg sphingomyelin) were simulated. Figure 1 shows the two types of phospholipid used in this study received from the cgmartini and Avantilipids webpages. DSPC and DPSM phospholipids are issued in the laboratory to synthesize spherical liposomes. The DSPC phospholipid creates spherical liposomal structures, while DPSM phospholipid develops a double layer membrane structure. Coarse-grained simulations consider similar atoms close together as a sphere, and allow simulations of systems that are not available at all common atomic time scales^{24,25}.

Results and Discussion

Today, many theoretical and empirical studies investigate the formation and stability of liposomes, due to their importance as drug carriers, and are experimentally synthesized in laboratories. However, molecular dynamics simulation has the ability to deliver more detailed information in the field of biosynthesis and drug delivering with regards to the high-cost of materials used for liposomes preparations, as well as limited documentation on stability of liposomes and its molecular arrangement²⁶. In fact, molecular dynamics simulation, as a primary study approach, helped to better investigate the liposomes formation process and stability. Using molecular dynamics simulation, the effect of different factors on the formation of liposomes and their stability was examined, so that an ideal liposome can be synthesized. In addition, the role and contribution of each interaction in the liposomes formation and stability can be evaluated. DSPC and DPSM Liposomes are experimentally synthesized and are the most important carriers as drug delivery system, including anticancer drugs. In this research, the main goal was to study the stability parameters and the DSPC and DPSM liposomes formation. The effective parameters in formulation and stability were extracted using data obtained from the simulation path file. The results showed differences in the formation and stability of DSPC and DPSM liposomes. In this study, in the self-assembly process, when the lipids are uniform and homogeneously distributed in water, the formation rate of liposomes is faster than when the lipids had bicelle clumps and other heterogeneous structures. The same results were reported by Chng *et al.* They examined the temperature effect on accelerating the formation of vesicles by DPPC lipid molecules caused by different water molecules per amphiphilic ratios. They concluded the binary associations between micelle-like lipids²⁷. Figure 2 shows the final structure of DSPC and DPSM liposomes after 1000 nanoseconds (1 microsecond). The results show that the DSPC lipid has two nanodisc structures and the DPSM lipid has three nanodisc structures in the simulation environment. The DSPC lipid has a cylindrical geometric structure and a small-sized head group that forms the spherical liposomal structure. On the other hand, the DPSM lipid has a conical geometric structure with a larger polar head group than another lipid, which allows the liposome to form a micelle structure. Although the DSPC and DPSM lipids used in the laboratory are always in liposome and micelle forms, they developed nanodisc structures in the simulation process²⁸.

The formation of liposomes. In this study, density, gyration radius, Radial Distribution Function (RDF), Root Mean Square Deviation (RMSD) and Solvent Accessible Surface Area (SASA) were employed to verify the liposomes formation^{29,30}. Using density analysis, the density profiles of lipid and water molecules were calculated along the Z direction. The density results reveal a nanodisc structures in the final stage^{31,32}. Figure 3(A1,A2,B1,B2) shows the density of lipid and water molecules. Figure 3(A1,B1) and Fig. 3(A2,B2) show the density of lipids and water molecules, respectively. The results reflect differences between lipid density profiles and water density in DSPC and DPSM lipids. According to Fig. 4B, the density of water molecules is low at the exact regions where the

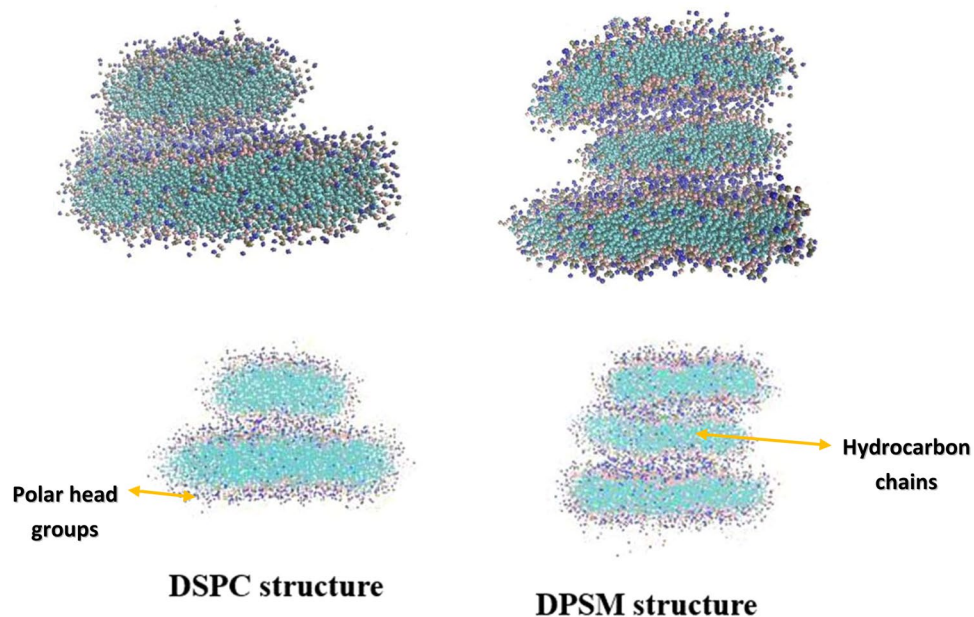


Figure 2. The final structure of lipids of DSPC and DPSM after 1000 nanoseconds (1 microsecond).

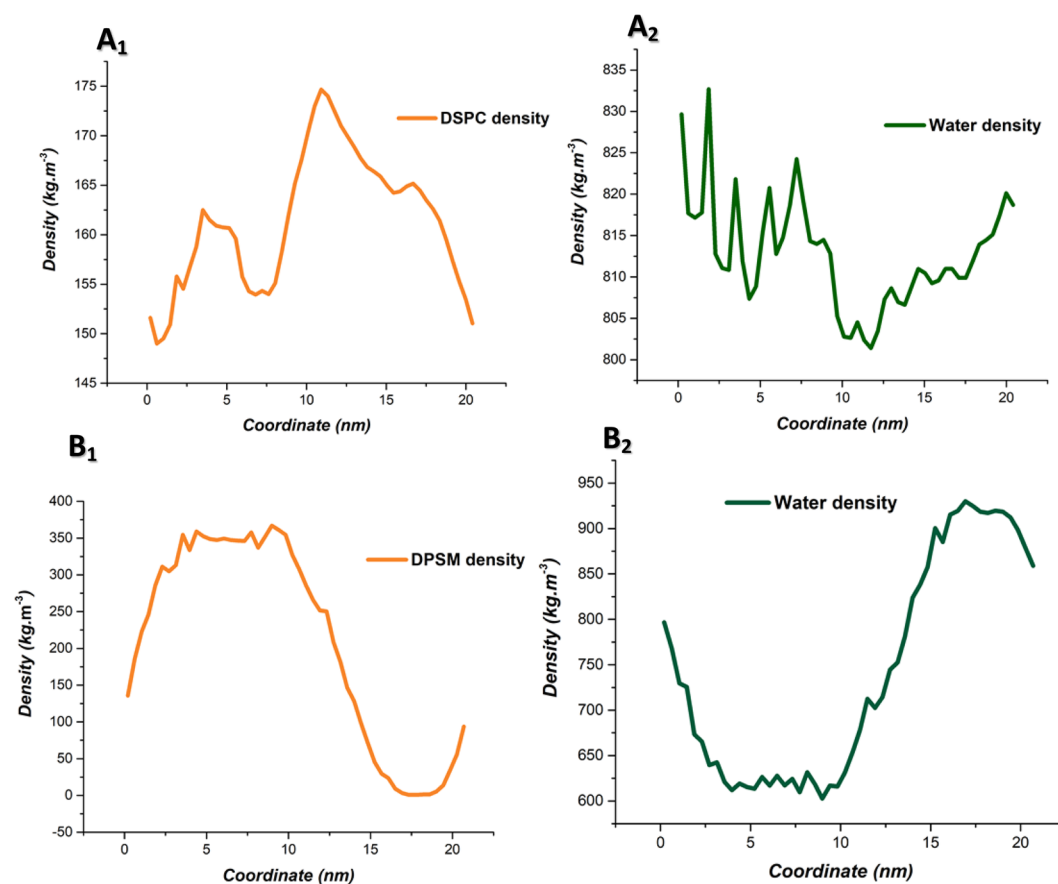


Figure 3. Density analysis shows that nanodisc structures have been created after simulation time. (A1) density of DSPC lipid molecules (A2) density of water molecules (B1) density of DPSM lipid molecules (B2) density of water molecules.

density of lipid molecules is high. The DSPC density profile shows a sharp peak in comparison with the DPSM lipid one, which could be related to different structure formations during self-assembly. Based on the results (Fig. 2), DSPC and DPSM are asymmetric and the lipids show an ordered cylindrical and spherical geometric structure.

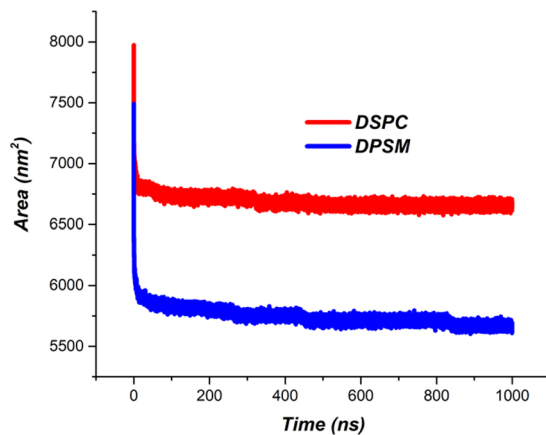


Figure 4. Solvent accessible surface area analysis for DSPC and DSPM liposome. The graph shows the amount of solvent.

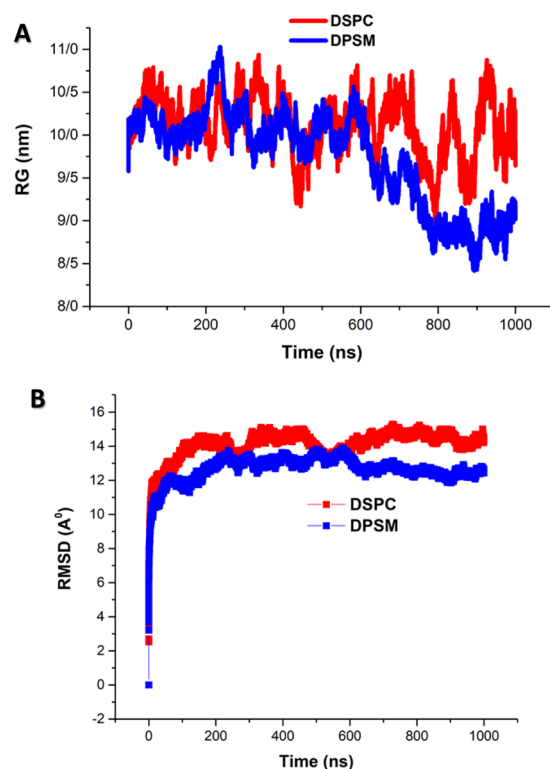


Figure 5. Radius of gyration and RMSD analysis during the simulation process.

In order to evaluate structural compression changes, the gyration radius diagram of each structure was recorded during the simulation time. The initial value of Rg for the DSPC and DSPM structures were 9.6 and 9.8 nm respectively. After completing the simulation and formation of nanodisc structures, analysis of the gyration radius of the total lipids was obtained. As shown in Fig. 5A, the analysis of the gyration radius shows that the DSPC and DSPM liposomes are compressed throughout the simulation time^{33,34}. In MD simulation, the gyration radius is an index to monitor the structural formation process³⁵. As shown in Fig. 5A, a sudden drop occurred in the gyration radius profile of the DSPC lipid which indicates structural transformation, while sharp and sudden drops and peaks are not observed in the DSPM lipids²⁶. The RMSD for each structure is based on its previous structure. Figure 5(B) shows the analysis of the RMSD parameter for the simulated lipid structures. As shown in Fig. 5(B), it is evident that the time required for attaining stable DSPC and DSPM structural formations is around 1 nanosecond, after which the RMSD reached a constant value after a few nanoseconds³⁶. Valeriya M. Trusova and *et al.*, reported a steady increase of RMSD value during the first 22 ns, and fluctuations were observed around

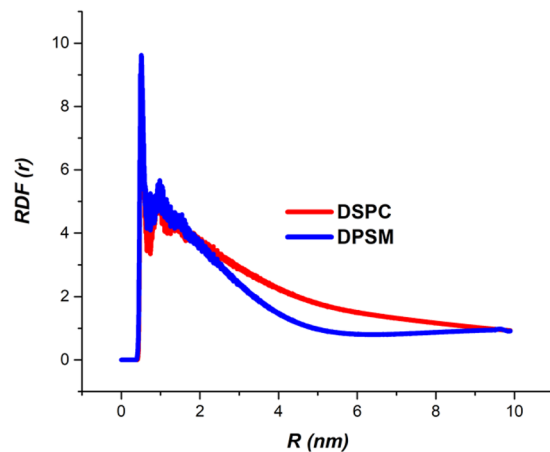


Figure 6. Radial distribution function analysis of DSPC and DPSM lipids. In both lipids, the source distance between the two side lipids is considered 0.5 nm.

an average value (i.e. ~ 0.21 ns). They concluded that the backbone RMSD value decreases due to partial unfolding. Moreover, lysozyme intramolecular leads to RMSD changes³⁷.

A Radial Distribution Function (RDF) is applied to describe the average structure of dynamic molecules and is a basic method for measuring the structure of a dense material³⁸. The RDF results show that DSPC and DPSM structures have a dense structure (Fig. 6). For better characterization of head group interaction, the RDF between the nitrogen (N4) in the choline and the phosphates (P8) at the two side of neighboring lipids in the head groups (DPSM and DSPC liposomes) were calculated³⁹. For calculation of the RDF in both liposomes, the source distance between the lipids was considered equal to 0.5 nm⁴⁰. The developed nanodiscs had an homogeneous structure and as a result, the RDF value increased at a certain distance (0.5 nm), followed by a significant reduction⁴¹. The distance between phosphate and nitrogen particles in the headgroups of DSPC and DPSM lipid molecules in a nanodisc display a sharp peak. The peak locations of the lipids headgroups correspond to the inner and outer radius of the nanodisc (see Fig. 6)⁴². It is likely that the DSPC and DPSM lipids are sufficiently equilibrated on such long time-scales (1000 ns). Choon-Peng Chng obtained partial equilibrated structures for monolayer lipids, suggesting longer simulation time to facilitate the flip-flops, as no flip-flops occurred during their simulations²⁷.

Solvent Accessible Surface Area (SASA) analysis was performed to verify the membrane and liposomal structural formation. Results from previous studies show that the amount of SASA is reduced by the formation of liposomes and membrane structures⁴³. As shown in Fig. 4, when the nanodiscs are formed, water penetration into the structures is prevented as a result. The results show that SASA values for the DSPC structure was higher than that of the DPSM structure (Fig. 4). The DSPC lipid has a low phase transition temperature and being more fluid at 400 °C, in turn leads to high SASA values. This issue reflects as increase in fluidity of the DSPC lipid and the weakening of the lipid packing as well as an increase in the space among them. In addition, analyzing the SASA is also used in investigation efforts on molecular structure and dynamics^{44–46}.

Energy analysis. Energy analyses (overall energy, Van der Waals and Electrostatic energies) was carried out to evaluate the energies and interactions contributing to the stability of the formed structures⁴⁷. To obtain the final stability state of liposomal structures, various energy analyses were conducted. The results of all energy analyses indicate the stability of the developed structures. According to the energy diagram, a decreasing system energy was observed due to the liposomal system formation during the simulation⁴⁸. Energy analysis was also performed at the equilibrium stage to check the stability of the system at this stage⁴⁹.

The effects of Van der Waals and Electrostatic energies on the stability of DSPC and DPSM liposomes. As shown in Fig. 7, the Van der Waals interactions were calculated for the liposomes. At the beginning of the simulation, the Van der Waals energy was low, but with the formation of Van der Waals interactions, its amount increased (became negative). The result showed that Van der Waals energy levels for the DPSM liposome are higher than that of the DSPC liposome, indicating greater amounts of Van der Waals interactions in this liposome. The nanodisc structure of the DPSM liposome makes it possible to produce more Van der Waals interactions⁵⁰.

Electrostatic interactions for both liposomes are presented in Fig. 8. It can be seen that Electrostatic energy levels for the DPSM liposome is higher than the DSPC liposome, indicating the greater number of Electrostatic interactions.

Study of stability of DSPC and DPSM liposomes using overall energy analysis. The final stability analysis of the developed structures was calculated using overall energy analysis. As shown in Figs. 7 and 8, the amount of Van der Waals and electrostatic energy for the DPSM Liposome are greater than that of the DSPC liposome. In Fig. 9, it is evident that the overall energy of the DPSM liposome is greater than that of the DSPC

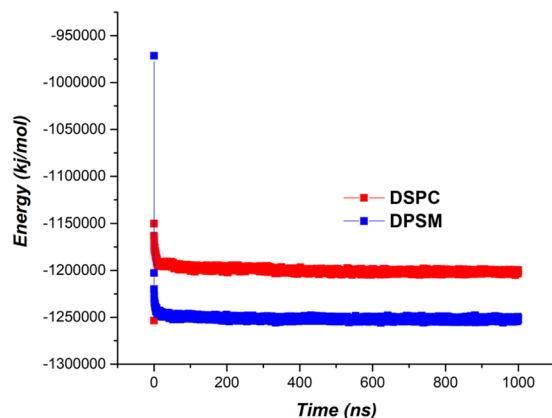


Figure 7. The energy of Van der Waals interactions for DPSM and DSPC liposomes.

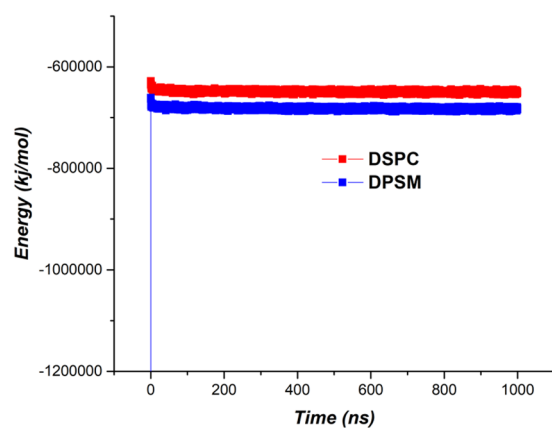


Figure 8. The energy of Electrostatic interactions for DPSM and DSPC liposomes.

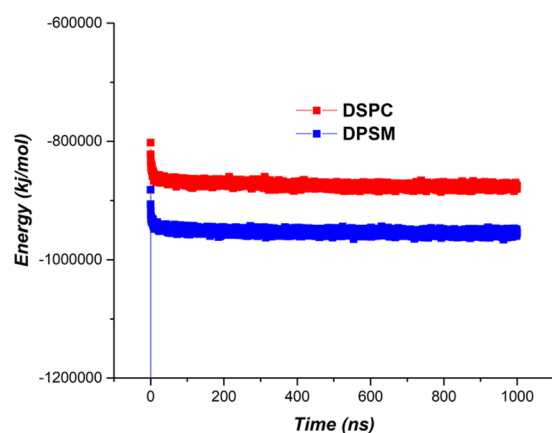


Figure 9. Overall energy of DPSM and DSPC liposomes.

liposome that have developed the nanodisc structure. As a result, the DPSM liposome is more stable than the DSPC liposome^{51–53}.

Conclusions

Liposomes carriers are widely used in biology and medicine and are implemented as carriers for many medications and biological molecules delivery. To reach high performances of the liposomes, they should be well-formed. Today, many theoretical and experimental studies investigate liposomes formation and stability. Molecular dynamics simulation, as a method of quantitative mathematical principles, is a complementary method to study the macromolecules mechanisms and dynamics, and biological phenomena. In this study, two types of liposomes

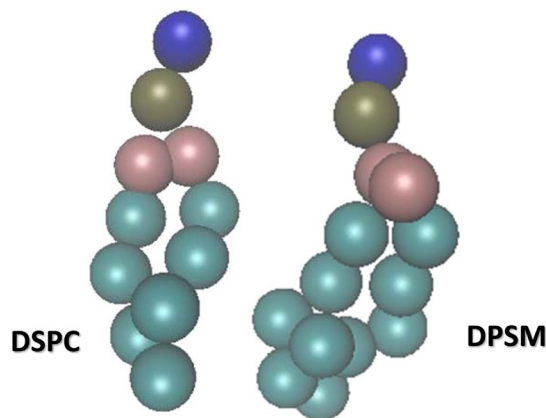


Figure 10. The coarse grain structure of 1,2-distearoyl-sn-glycero-3-phosphocholine and Egg sphingomyelin phospholipids obtained from CHARMM site.

were simulated to investigate their formation and stability. Self-assembly approaches of two types of phospholipid, namely, DSPC and DPSM, from random initial configuration was simulated. The MARTINI coarse-grain model and GROMACS package was employed in this study. The simulations reveal that there is one basic self-assembled structure, i.e. the nanodisc structure. Formation analyses, including density, radial distribution function, solvent accessible surface area, gyration radius, and root mean square deviation were applied. The formation analyses showed that the DSPC lipid has two structures of nanodisc while the DPSM lipids have three nanodisc structures in the simulation environment. It seems that the physicochemical properties have a pivotal role in the structure of each liposome in terms of structural formation and stability. The DSPC lipid had a cylindrical geometric structure and a small-sized head group originally, that forms the bilayer structure. Meanwhile, the DPSM lipid had a conical geometric structure and has also a larger head group than other lipids, which allows the liposome to form a micelle structure. Although DSPC and DPSM lipids are used in the laboratory and produce liposome and micelle, they have developed nanodisc structures in this study. In addition, to check the stability of the developed structures, energy analyses including Van der Waals interactions, electrostatic interactions, and overall energy interactions were performed. All the energy analyses indicate that the DPSM liposome was more stable than the DSPC liposome. RMSD and energy profile results for these structures indicated their stability. Bilayer, micelles, hexagonal structures and etc., can be formed during the simulation process of lipids. The results of energy profile analysis confirmed this hypothesis that the nanodisc structure is more stable than other formation. Regarding the timescales of the simulations presented in this study (1000 ns), headgroup-headgroup binding of lipids improved the Van der Waals and Electrostatic interactions significantly.

Arnarez *et al.*²³, introduced a novel Coarse-Grained Martini model, “Dry” Martini. They showed that, their model is able to study the lipid membrane properties including bilayer thickness, area per lipid, bending modulus, and coexistence of liquid-ordered and disordered domains. Moreover, they showed that the Dry Martini can be used to study membrane fusion and formation of tether, with results similar to those of the standard Martini model. By this model, they noted that the membrane proteins could also be investigated, but less quantitative results they obtained. In comparison with current study, one of the most important aspect of MD simulation is speedups for large systems. Arnarez *et al.*, in their study concluded that the absence of water in Dry Martini leads to a significant speedup for large systems, and suggested the new model is able to the study of complex multi-component membranes containing millions of lipids. The results of this study provided significant evidence for the importance of the molecular dynamics simulations on the structural stability and mechanisms of formation of DSPC and DPSM lipids, these can be useful as a guide to the experimental synthesis of these lipids. The results of this simulations study revealed that, bilayer nanodisc structures are stable than others structures, which could help to design of lipids like liposome with high efficacy for pharmaceutical applications.

Materials and Methods

In this research, the formation and stability of the phospholipids were investigated in the simulation environment⁵⁴. The time scale was considered at the microsecond. In the martini model, there are four types of atoms including Apolar (C), Polar (P), Non-polar (N) and Charged (Q)⁵⁵. DSPC phospholipids includes grains of NC31 (blue color), PO4 (gray), GL1 and GL2 (pink), C1Am, C2A, C3A, C4A, C5A, C1B, C2B, C3B, C4B and C5B (turquoise blue). And Dpsm phospholipids includes grains of NC3 (blue), PO4 (gray), AM1 and AM2 (pink), T1A, C2A, C3A, C1B, C2B, C3B and C4B (turquoise color). The initial data of the phospholipid components (including phospholipids of 1,2-distearoyl-sn-glycero-3-phosphocholine and Egg sphingomyelin) were obtained as a coarse grain state from the web server CHARMM-gui (<http://www.charmm-gui.org/>) (Fig. 10). CHARMM-gui was used for the construction of initial structures of the phospholipids and then simulations were carried out using the Gromacs software (version 5.0.1)⁵⁶. The main parameter files (*i.e.* ITP and TOP files), which are required to initiate the simulation process in the Gromacs environment, was taken from the CHARMM-gui website^{26,57}.

Creating the boxes and hydration of phospholipids. In this study, each phospholipid molecule was placed randomly in a cube-shaped box of 20 nm dimensions. A certain number of phospholipid molecules was

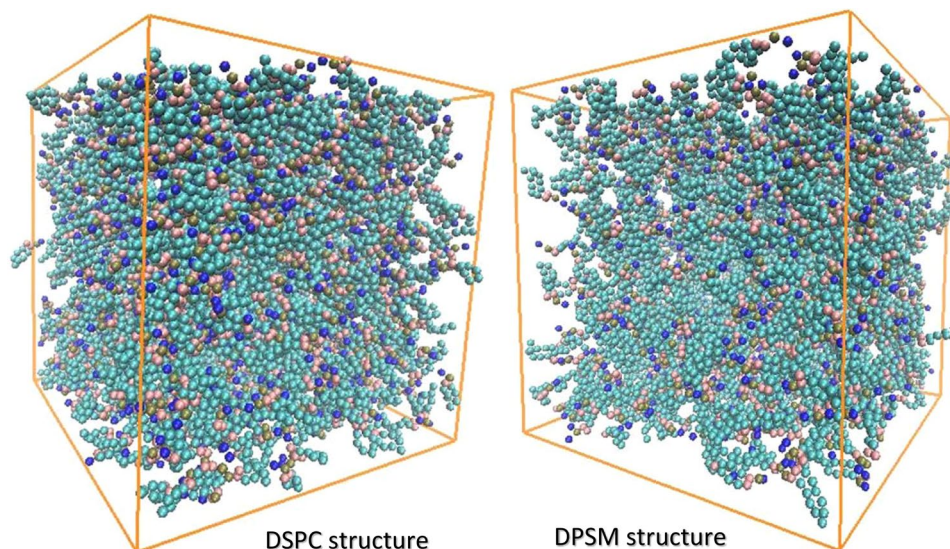


Figure 11. Simulation box and initial configuration defined for DSPC and DPSM lipids. For the DSPC liposome, 901 molecules 1,2-distearoyl-sn-glycero-3-phosphocholine and 60311 molecules of water, and for the DPSM liposome, 901 molecules of Egg sphingomyelin and 60311 molecules of water were placed in the box.

added to each of the box systems (Fig. 11). For the DSPC liposome, 901 molecules 1,2-distearoyl-sn-glycero-3-phosphocholine and 60311 molecules of water, and for the DPSM liposome, 901 molecules of Egg sphingomyelin and 60311 molecules of water were placed in the box. The parameters used in this study were provided based on the proportions and concentration results from previous research works, reported for the liposome synthesis. Water molecules were added to the system for watering. The type of water used in this research was coarse-grain and polarized Martini model^{22,58–60}.

Molecular dynamics simulation studies. In this study, two molecular dynamics simulation processes were performed for DSPC and DPSM liposomes. The simulation time for each liposome was 1,000 nanoseconds (1 microsecond). All simulations were performed using the Gromacs software and Martini force field 2.2.^{61–63} Energy minimization steps were equal to 3000 steps and equilibrium in constant volume to adjust the temperature at 400 Kelvin and equilibrium at constant pressure to adjust the pressure, at atmospheric pressure (1 bar). Besides, the time step was set 20 femtoseconds^{64–66}.

The mdp file entries were also set. The nst list parameter was set equal to 10. The coulomb-type and vdw_type parameters are defined as cut-offs, and the algorithms were respectively defined for the t-coupl, p-coupl and cutoff-scheme parameters including v-rescale, berendsen and verlet.

Results analysis of molecular dynamics simulation. After completing the MD simulation steps, the results were recorded in the output files (EDR, TPR, XTC, GRO, etc.). The results were used to investigate the formation and stability of liposomal structures, including analysis of density, gyration radius, radial distribution function, and solvent accessible surface area. An overall energy analysis was also carried out.

Received: 29 October 2019; Accepted: 19 January 2020;

Published online: 04 February 2020

References

- Peer, D. *et al.* Nanocarriers as an emerging platform for cancer therapy. *Nature nanotechnology* **2**, 751 (2007).
- Wu, G., Mikhailovsky, A., Khant, H. A. & Zasadzinski, J. A. Synthesis, characterization, and optical response of gold nanoshells used to trigger release from liposomes. *Methods in enzymology* **464**, 279–307 (2009).
- Anderson, L. J., Hansen, E., Lukianova-Hleb, E. Y., Hafner, J. H. & Lapotko, D. O. Optically guided controlled release from liposomes with tunable plasmonic nanobubbles. *Journal of Controlled Release* **144**, 151–158 (2010).
- Liu, Z., Winters, M., Holodniy, M. & Dai, H. siRNA delivery into human T cells and primary cells with carbon-nanotube transporters. *Angewandte Chemie International Edition* **46**, 2023–2027 (2007).
- Steger, L. D. & Desnick, R. J. Enzyme therapy VI: Comparative *in vivo* fates and effects on lysosomal integrity of enzyme entrapped in negatively and positively charged liposomes. *Biochimica et Biophysica Acta (BBA)-Biomembranes* **464**, 530–546 (1977).
- Finkelstein, M. & Weissmann, G. The introduction of enzymes into cells by means of liposomes. *Journal of lipid research* **19**, 289–303 (1978).
- Shen, Z. *et al.* Polymer stiffness governs template mediated self-assembly of liposome-like nanoparticles: simulation, theory and experiment. *Nanoscale* **11**, 20179–20193, <https://doi.org/10.1039/C9NR07063J> (2019).
- Marchetti, B. & Abbracchio, M. P. To be or not to be (inflamed)—is that the question in anti-inflammatory drug therapy of neurodegenerative disorders? *Trends in pharmacological sciences* **26**, 517–525 (2005).
- Shen, Z. *et al.* Self-assembly of core-polyethylene glycol-lipid shell (CPLS) nanoparticles and their potential as drug delivery vehicles. *Nanoscale* **8**, 14821–14835 (2016).

10. Chan, P. H., Longar, S. & Fishman, R. A. Protective effects of liposome-entrapped superoxide dismutase on posttraumatic brain edema. *Annals of Neurology: Official Journal of the American Neurological Association and the Child Neurology Society* **21**, 540–547 (1987).
11. Miller, A. D. Cationic liposomes for gene therapy. *Angewandte Chemie International Edition* **37**, 1768–1785 (1998).
12. Sharma Vijay, K., Mishra, D., Sharma, A. & Srivastava, B. Liposomes: present prospective and future challenges. *International Journal of Current Pharmaceutical Review & Research* **1**, 6–16 (2010).
13. Ugwu, S. *et al.* Preparation, characterization, and stability of liposome-based formulations of mitoxantrone. *Drug development and industrial pharmacy* **31**, 223–229 (2005).
14. Kawakami, K., Nishihara, Y. & Hirano, K. Effect of hydrophilic polymers on physical stability of liposome dispersions. *The Journal of Physical Chemistry B* **105**, 2374–2385 (2001).
15. Shen, Z., Ye, H., Kröger, M. & Li, Y. Aggregation of polyethylene glycol polymers suppresses receptor-mediated endocytosis of PEGylated liposomes. *Nanoscale* **10**, 4545–4560 (2018).
16. Wagner, A., Vorauer-Uhl, K. & Katinger, H. Liposomes produced in a pilot scale: production, purification and efficiency aspects. *European Journal of Pharmaceutics and Biopharmaceutics* **54**, 213–219 (2002).
17. Sharma, A. *et al.* Activity of paclitaxel liposome formulations against human ovarian tumor xenografts. *International journal of cancer* **71**, 103–107 (1997).
18. Rigacci, L. *et al.* Liposome-encapsulated doxorubicin in combination with cyclophosphamide, vincristine, prednisone and rituximab in patients with lymphoma and concurrent cardiac diseases or pre-treated with anthracyclines. *Hematological oncology* **25**, 198–203 (2007).
19. Hong, J. S. *et al.* Microfluidic directed self-assembly of liposome– hydrogel hybrid nanoparticles. *Langmuir* **26**, 11581–11588 (2010).
20. Shen, Z., Ye, H., Kröger, M., Tang, S. & Li, Y. Interplay between ligand mobility and nanoparticle geometry during cellular uptake of PEGylated liposomes and bicelles. *Nanoscale* **11**, 15971–15983, <https://doi.org/10.1039/C9NR02408E> (2019).
21. Müller, R. H., Mäder, K. & Gohla, S. Solid lipid nanoparticles (SLN) for controlled drug delivery—a review of the state of the art. *European journal of pharmaceutics and biopharmaceutics* **50**, 161–177 (2000).
22. Arifin, D. R. & Palmer, A. F. Stability of liposome encapsulated hemoglobin dispersions. *Artificial cells, blood substitutes, and biotechnology* **33**, 113–136 (2005).
23. Arnarez, C. M. *et al.* Dry Martini, a coarse-grained force field for lipid membrane simulations with implicit solvent. *Journal of Chemical Theory and Computation* **11**, 260–275 (2014).
24. Mugabe, C., Azghani, A. O. & Omri, A. Liposome-mediated gentamicin delivery: development and activity against resistant strains of *Pseudomonas aeruginosa* isolated from cystic fibrosis patients. *Journal of Antimicrobial Chemotherapy* **55**, 269–271 (2005).
25. Sun, F. *et al.* Dimerization and structural stability of amyloid precursor proteins affected by the membrane microenvironments. *Journal of chemical information and modeling* **57**, 1375–1387 (2017).
26. Ingram, T. *et al.* Prediction of micelle/water and liposome/water partition coefficients based on molecular dynamics simulations, COSMO-RS, and COSMOmic. *Langmuir* **29**, 3527–3537 (2013).
27. Chng, C.-P. Effect of simulation temperature on phospholipid bilayer–vesicle transition studied by coarse-grained molecular dynamics simulations. *Soft Matter* **9**, 7294–7301 (2013).
28. Li, J. *et al.* A review on phospholipids and their main applications in drug delivery systems. *Asian journal of pharmaceutical sciences* **10**, 81–98 (2015).
29. Magarkar, A., Rog, T. & Bunker, A. Molecular dynamics simulation of PEGylated membranes with cholesterol: building toward the DOXIL formulation. *The Journal of Physical Chemistry C* **118**, 15541–15549 (2014).
30. Matsuoka, K. *et al.* COPII-coated vesicle formation reconstituted with purified coat proteins and chemically defined liposomes. *Cell* **93**, 263–275 (1998).
31. Risselada, H. J. & Marrink, S. J. Curvature effects on lipid packing and dynamics in liposomes revealed by coarse grained molecular dynamics simulations. *Physical Chemistry Chemical Physics* **11**, 2056–2067 (2009).
32. Uster, P. S. *et al.* Insertion of poly (ethylene glycol) derivatized phospholipid into pre-formed liposomes results in prolonged *in vivo* circulation time. *FEBS letters* **386**, 243–246 (1996).
33. Chun, B. J., Choi, J. I. & Jang, S. S. Molecular dynamics simulation study of sodium dodecyl sulfate micelle: Water penetration and sodium dodecyl sulfate dissociation. *Colloids and Surfaces A: Physicochemical and Engineering Aspects* **474**, 36–43 (2015).
34. Fixman, M. Radius of gyration of polymer chains. *The Journal of Chemical Physics* **36**, 306–310 (1962).
35. Stevens, M. J., Hoh, J. H. & Woolf, T. B. Insights into the molecular mechanism of membrane fusion from simulation: evidence for the association of splayed tails. *Physical review letters* **91**, 188102 (2003).
36. Galeazzi, R. *et al.* Liposome-based gene delivery systems containing a steroid derivative: computational and small angle X-ray diffraction study. *RSC Advances* **5**, 54070–54078 (2015).
37. Trusova, V. M. & Gorbenko, G. P. Molecular dynamics simulations of lysozyme–lipid systems: probing the early steps of protein aggregation. *Journal of Biomolecular Structure and Dynamics* **36**, 2249–2260 (2018).
38. Levine, B. G., Stone, J. E. & Kohlmeyer, A. Fast analysis of molecular dynamics trajectories with graphics processing units—Radial distribution function histogramming. *Journal of Computational Physics* **230**, 3556–3569 (2011).
39. Pandit, S. A., Jakobsson, E. & Scott, H. Simulation of the early stages of nano-domain formation in mixed bilayers of sphingomyelin, cholesterol, and dioleoylphosphatidylcholine. *Biophysical journal* **87**, 3312–3322 (2004).
40. Leekumjorn, S. *et al.* The role of fatty acid unsaturation in minimizing biophysical changes on the structure and local effects of bilayer membranes. *Biochimica et Biophysica Acta (BBA)-Biomembranes* **1788**, 1508–1516 (2009).
41. Corsi, J., Hawtin, R. W., Ces, O., Attard, G. S. & Khalid, S. DNA lipoplexes: formation of the inverse hexagonal phase observed by coarse-grained molecular dynamics simulation. *Langmuir* **26**, 12119–12125 (2010).
42. Jalili, S. & Saeedi, M. Study of curcumin behavior in two different lipid bilayer models of liposomal curcumin using molecular dynamics simulation. *Journal of Biomolecular Structure and Dynamics* **34**, 327–340 (2016).
43. Hasel, W., Hendrickson, T. F. & Still, W. C. A rapid approximation to the solvent accessible surface areas of atoms. *Tetrahedron Computer Methodology* **1**, 103–116 (1988).
44. Tirosh, O., Barenholz, Y., Katzhendler, J. & Prieve, A. Hydration of polyethylene glycol-grafted liposomes. *Biophysical journal* **74**, 1371–1379 (1998).
45. Hamed, E., Xu, T. & Ketten, S. Poly (ethylene glycol) conjugation stabilizes the secondary structure of α -helices by reducing peptide solvent accessible surface area. *Biomacromolecules* **14**, 4053–4060 (2013).
46. Zhang, M. *et al.* HDL surface lipids mediate CETP binding as revealed by electron microscopy and molecular dynamics simulation. *Scientific reports* **5**, 8741 (2015).
47. Zou, P., Bortolus, M. & Mchaourab, H. S. Conformational cycle of the ABC transporter MsbA in liposomes: detailed analysis using double electron–electron resonance spectroscopy. *Journal of molecular biology* **393**, 586–597 (2009).
48. Mohammed, A., Weston, N., Coombes, A., Fitzgerald, M. & Perrie, Y. Liposome formulation of poorly water soluble drugs: optimisation of drug loading and ESEM analysis of stability. *International journal of pharmaceutics* **285**, 23–34 (2004).
49. Mugabe, C., Halwani, M., Azghani, A. O., Lafrenie, R. M. & Omri, A. Mechanism of enhanced activity of liposome-entrapped aminoglycosides against resistant strains of *Pseudomonas aeruginosa*. *Antimicrobial agents and chemotherapy* **50**, 2016–2022 (2006).

50. Bhattacharya, S. & Haldar, S. Interactions between cholesterol and lipids in bilayer membranes. Role of lipid headgroup and hydrocarbon chain–backbone linkage. *Biochimica et Biophysica Acta (BBA)-Biomembranes* **1467**, 39–53 (2000).
51. Seydel, J. K. & Wiese, M. *Drug-membrane interactions: analysis, drug distribution, modeling*. Vol. 15 (John Wiley & Sons, 2009).
52. Tantakitti, F. *et al.* Energy landscapes and functions of supramolecular systems. *Nature materials* **15**, 469 (2016).
53. Xiang, T.-X. & Anderson, B. D. Liposomal drug transport: a molecular perspective from molecular dynamics simulations in lipid bilayers. *Advanced drug delivery reviews* **58**, 1357–1378 (2006).
54. Cheng, X., Jo, S., Lee, H. S., Klauda, J. B. & Im, W. (ACS Publications, 2013).
55. Qi, Y. *et al.* CHARMM-GUI martini maker for coarse-grained simulations with the martini force field. *Journal of chemical theory and computation* **11**, 4486–4494 (2015).
56. Qi, Y. *et al.* CHARMM-GUI PACE CG Builder for solution, micelle, and bilayer coarse-grained simulations. *Journal of chemical information and modeling* **54**, 1003–1009 (2014).
57. Uemura, A., Kimura, S. & Imanishi, Y. Investigation on the interactions of peptides in the assembly of liposome and peptide by fluorescence. *Biochimica et Biophysica Acta (BBA)-Biomembranes* **729**, 28–34 (1983).
58. Gao, H., Zhang, Q., Yu, Z. & He, Q. Cell-penetrating peptide-based intelligent liposomal systems for enhanced drug delivery. *Current pharmaceutical biotechnology* **15**, 210–219 (2014).
59. Geers, B. *et al.* Targeted liposome-loaded microbubbles for cell-specific ultrasound-triggered drug delivery. *Small* **9**, 4027–4035 (2013).
60. Shinoda, W., DeVane, R. & Klein, M. L. Computer simulation studies of self-assembling macromolecules. *Current Opinion in Structural Biology* **22**, 175–186 (2012).
61. Shih, C.-J., Lin, S., Sharma, R., Strano, M. S. & Blankschtein, D. Understanding the pH-dependent behavior of graphene oxide aqueous solutions: a comparative experimental and molecular dynamics simulation study. *Langmuir* **28**, 235–241 (2011).
62. Friedrichs, M. S. *et al.* Accelerating molecular dynamic simulation on graphics processing units. *Journal of computational chemistry* **30**, 864–872 (2009).
63. Rapaport, D. C. & Rapaport, D. C. R. *The art of molecular dynamics simulation*. (Cambridge university press, 2004).
64. Allen, M. P. Computational Soft Matter: From Synthetic Polymers to Proteins. *Lecture Notes*, 1–28 (2004).
65. Cuendet, M. Molecular dynamics simulation. *European Molecular Biological Laboratory*, 1–67 (2008).
66. Izvekov, S. & Voth, G. A. A multiscale coarse-graining method for biomolecular systems. *The Journal of Physical Chemistry B* **109**, 2469–2473 (2005).

Author contributions

H.H., H.J. and M.H.D. contributed equally to this work. H.H. and M.H.D. conceived and performed the experiments; H.J. analyzed the data; H.H. prepared the figures; H.H., H.J. and M.H.D. wrote the manuscript.

Competing interests

The authors declare no competing interests.

Additional information

Correspondence and requests for materials should be addressed to M.H.D.

Reprints and permissions information is available at www.nature.com/reprints.

Publisher's note Springer Nature remains neutral with regard to jurisdictional claims in published maps and institutional affiliations.



Open Access This article is licensed under a Creative Commons Attribution 4.0 International License, which permits use, sharing, adaptation, distribution and reproduction in any medium or format, as long as you give appropriate credit to the original author(s) and the source, provide a link to the Creative Commons license, and indicate if changes were made. The images or other third party material in this article are included in the article's Creative Commons license, unless indicated otherwise in a credit line to the material. If material is not included in the article's Creative Commons license and your intended use is not permitted by statutory regulation or exceeds the permitted use, you will need to obtain permission directly from the copyright holder. To view a copy of this license, visit <http://creativecommons.org/licenses/by/4.0/>.

© The Author(s) 2020